

# **Experimental and Modeling Study of Double-layered UHPFRC under Bending**

## **Author(s) & Affiliation:**

**Y.Y.Y. Cao\***(corresponding author)- Department of the Built Environment, Eindhoven University of Technology, 5600 MB Eindhoven, the Netherlands, Email: y.cao.1@tue.nl

**Q.L. Yu**- Assistant Professor, Department of the Built Environment, Eindhoven University of Technology, P.O. Box 513, 5600 MB Eindhoven, the Netherlands, Email: q.yu.1@tue.nl

**H.J.H. Brouwers**- Professor, Department of the Built Environment, Eindhoven University of Technology, P.O. Box 513, 5600 MB Eindhoven, the Netherlands, Email: jos.brouwers@tue.nl

**Abstract:** Ultra-High Performance Fiber Reinforced Concrete (UHPFRC) is a material characterized by very high compressive strength, excellent durability and damage tolerance. For a UHPFRC beam works under bending, steel fibers distributed in the beam compressive zone has insignificant effects on the improvement of its flexural capacity. To use the fibers more efficiently, this paper applies the concept of layered-structure to UHPFRC beam. A double-layered UHPFRC beam composed of a top plain UHPC layer and a bottom UHPFRC layer containing 2% steel fibers is designed. In the experimental section, basic mechanical properties of the individual UHPC and UHPFRC layers are investigated. Compression, split tension and bending tests are conducted, the results of which provide input parameters and model validation for the simulation section. The effects of layer thickness on the beam flexural properties and stress distributions are analyzed numerically with the validated model, and the results show that the peak flexural load and the energy increase with the increase of the UHPFRC layer thickness. Results from this study shed lights on the design of layered UHPFRC structures, and contribute to the application of layered UHPFRC in engineering constructions.

**Keywords:** Layered structure; cementitious composite; ultra-high performance concrete; flexural bending; numerical simulation.

## **1. Introduction**

Ultra-high performance fiber reinforced concrete (UHPFRC) is a construction material with advanced mechanical properties [1]: the compressive strength, durability and energy absorption capacities are superior to those of the traditional concrete. Generally, UHPFRC can be seen as a composite made of Ultra-high performance concrete (UHPC) matrix and steel fibers. The application of fibers to the UHPC matrix has been recognized to significantly enhance the tensile properties of UHPFRC. However, steel fibers are reported to have insignificant contributions on increasing the compressive strength of UHPFRC [2]. As a result, fibers are not fully utilized in some structures which contain both tension and compression zones. One typical example is a bending beam. When a beam is working under service situations, half of it is in compression while the other half is in tension. Steel fibers in the tensile zone improve the flexural performances of the beam, while those in the compressive zone have no apparent effects [3]. Consequently, a

homogeneous UHPFRC with fibers distributed in the whole structure fails to use the fibers effectively. To generate a more efficient utilization of the fibers, a layered UHPFRC beam with fibers purposefully reinforced in the targeted region is preferred.

The flexural performance under three-point bending is often applied as an indicator to evaluate the load carrying capacity and the fracture toughness of cementitious material [4,5]. Current researches on the flexural behavior of UHPFRC mainly focus on the homogeneous type. Yoo et al. [6] studied the flexural behavior of UHPFRC and found that its post-cracking performance was improved with an increase in fiber amount. Kim et al. [7] investigated the influences of micro-fiber content in UHPFRC with hybrid fibers. Their results exhibited that the load carrying capacity, the deflection capacity and the energy absorption capacity were improved as the micro-fiber content increases. Despite the studies on homogeneous UHPFRC, there is still a lack of systematic research on the flexural response of layered UHPFRC, and influences of the layer thickness on the flexural strength and toughness are not clear.

To bridge the gap, this paper conducts investigations on a designed double-layered UHPFRC beam composed of a top plain UHPC layer and a bottom UHPFRC layer. The paper includes two sections, i.e. an experimental one and a numerical one. Basic properties of the UHPC and the UHPFRC materials are investigated by experiments first, which provide input parameters and validations for the following simulations. Then, the bending behavior of the double-layered UHPFRC beam is analyzed numerically. The effects of increasing UHPFRC layer thickness on the enhancement of the beam flexural performance, and on the stress distributions at both elastic stage and inelastic stages are discussed. The results from this study contribute to a better understanding of the flexural behavior of layered UHPFRC as well as to promote a more efficient utilization of the steel fibers.

## **2. Experimental program**

In this section, mix designs of the UHPC and the UHPFRC are given, and their basic mechanical properties are tested. The material density, elastic modulus, tensile and compressive strengths obtained in this section are used as inputs for the numerical simulations in the next section; and the flexural performances of the UHPC and the UHPFRC provide validation for the simulations as well.

### ***2.1. Materials and sample preparation***

Recipes of the UHPC and the UHPFRC are presented in Table 1. Portland cement CEM I 52.5 R, micro-silica, limestone powder, sand, basalt aggregate, superplasticizer and water are utilized for the UHPC. 2% straight steel fibers (length = 13 mm, diameter = 0.2 mm, tensile strength = 2750 MPa) are added to produce the UHPFRC. The water binder ratio for the UHPC and the UHPFRC are 0.19 and 0.23, respectively. More water is added in the UHPFRC to ensure its flowability.

The mixing procedure was conducted at room temperature: dry mixing of all powders and the sand for two minutes; adding 75% of the water and mixing for another two minutes; adding the superplasticizer with the remaining water and mixing for four minutes; sequentially adding the basalt aggregates and mix for three minutes. Steel fibers were added and mixed for three more minutes in the case of UHPFRC. After the mixing procedure, the mixture was poured into moulds to cast the UHPC and the UHPFRC samples. The casted samples were covered with plastic sheets for 24 hours. Then they were demolded and cured in water at the room temperature for additional 27 days.

**Table 1 Recipes of the UHPC and the UHPFRC: CEM = Portland cement, mS = micro-silica, LP = limestone powder, S = sand, BA 2-5 = basalt aggregate with a diameter of 2-5 mm, BA 5-8 = basalt aggregate with a diameter of 5-8 mm, SP = superplasticizer, W = water, SF = steel fiber.**

| Materials | CEM<br>(kg/m <sup>3</sup> ) | mS<br>(kg/m <sup>3</sup> ) | LP<br>(kg/m <sup>3</sup> ) | S<br>(kg/m <sup>3</sup> ) | BA 2-5<br>(kg/m <sup>3</sup> ) | BA 5-8<br>(kg/m <sup>3</sup> ) | SP<br>(kg/m <sup>3</sup> ) | W<br>(kg/m <sup>3</sup> ) | SF<br>(%) |
|-----------|-----------------------------|----------------------------|----------------------------|---------------------------|--------------------------------|--------------------------------|----------------------------|---------------------------|-----------|
| UHPC      | 588.0                       | 39.2                       | 156.8                      | 839.9                     | 413.2                          | 232.3                          | 10.2                       | 149.0                     | 0.0       |
| UHPFRC    |                             |                            |                            |                           |                                |                                |                            | 180.3                     | 2.0       |

## 2.2. Test methods

The compressive and the splitting tensile strengths of the casted UHP(FR)C samples were measured using 100×100×100 mm<sup>3</sup> cubes based on EN 12390-3 [8] and EN 12390-6 [9] standards, respectively. Moreover, the elastic modulus of the UHPC and the UHPFRC materials were tested with beams (100×100×500 mm<sup>3</sup>) according to ASTM C 469-02 [10]. A universal testing machine with a maximum load capacity of 4000 kN was utilized for the tests.

Three-point bending tests of the homogeneous UHPC and UHPFRC beams were conducted at the age of 28 days. The dimensions of the beam were 100×100×500 mm<sup>3</sup> and the span length was 400 mm [11]. The tests were performed with an Instron 5985 testing machine under displacement control at the rate of 0.2 mm/min [12]. The mid-point deflections of the beams were measured with two linear variable differential transducers (LVDTs).

## 2.3. Test results

Table 2 gives the basic properties of the UHPC and the 2% fiber UHPFRC materials. It can be seen from the table that the UHPC and the UHPFRC materials have a similar density and elastic modulus, indicating the slight effects of steel fibers on these properties. On the contrary, the tensile strength is higher for the UHPFRC with 2% fibers, which is attributed to the efficiency of fibers to connect cracks. The compressive strength of the UHPFRC is slightly smaller compared with that of the UHPC. This is due to the higher water/binder ratio of the UHPFRC mixture in order to achieve a satisfying flowability.

Data given in Table 2 are further used as model inputs in the next simulation section. Additionally, it should be noted that the flexural properties of the UHPC and UHPFRC beams under three-point bending tests are not given in this experimental section. Instead, they are presented and compared in the simulation section as a validation of the material models.

**Table 2 Basic properties of the UHPC and the UHPFRC:  $\rho$  = density,  $f_c$  = compressive strength,  $f_t$  = split tensile strength,  $E$  = elastic modulus**

| Materials | $\rho$ (kg/m <sup>3</sup> ) | $f_c$ (MPa) | $f_t$ (MPa) | $E$ (GPa) |
|-----------|-----------------------------|-------------|-------------|-----------|
| UHPC      | 2540                        | 143.0       | 9.03        | 53.5      |
| UHPFRC    | 2560                        | 138.9       | 13.9        | 51.3      |

## 3. Numerical simulation

In this section, simulations of the homogenous UHPC and the 2% fiber UHPFRC beams under three-point bending are conducted. Material model inputs with regard to basic material properties are obtained from the tests in Section 2, and the numerical models are validated by comparing the simulation results with the experimental ones. After validating the numerical models, simulations of double-layered beams are conducted to reveal the effects of the layer thickness.

### 3.1 Model development

3D modellings of the three-point bending tests are constructed in ANSYS/LS-DYNA. Both homogeneous and layered beams are simulated. An example of the double-layered UHPFRC beam model is presented in Fig.1.

Solid elements are used in the model, and the smallest mesh size is 5 mm. The contact between the steel rollers and the beam is described using the automatic surface to surface algorithm. The loading on the beam is achieved by setting the velocity of the top steel roller using the option “BOUNDARY\_PRESCRIBED\_MOTION\_SET”.

For the steel rollers, a basic plastic kinematic model is adopted due to its simplicity and adequate accuracy [13]. For the UHPC and the UHPFRC materials, RHT model is employed. This model is developed for brittle material and it is particularly useful for describing the damage and plastic behaviors of concrete [13]. More information on the mechanical properties of the RHT model can be found in [13,14].

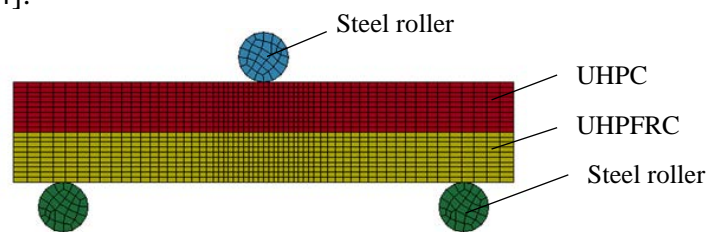


Fig. 1 Model of the three point bending test

### 3.2 Model validation

The bending behaviors of the plain UHPC and the 2% fiber UHPFRC beams are simulated first and compared with the experimental results for model validations. Fig.2 illustrates the flexural load-displacement curves of the UHPC and the UHPFRC. In addition, the numerical and the experimental cracking patterns of the UHPFRC beam are compared in Fig.3. It can be observed from Figs.2 and 3 that the simulation results agree well with the experimental ones, indicating the appropriation of the applied material models and the input parameters. Therefore, these material models and parameters are further utilized to simulate the bending behavior of the double-layered UHPFRC beam, and effects of the layer thickness are discussed numerically.

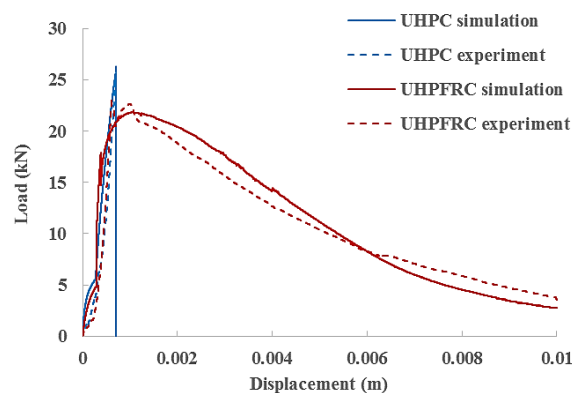
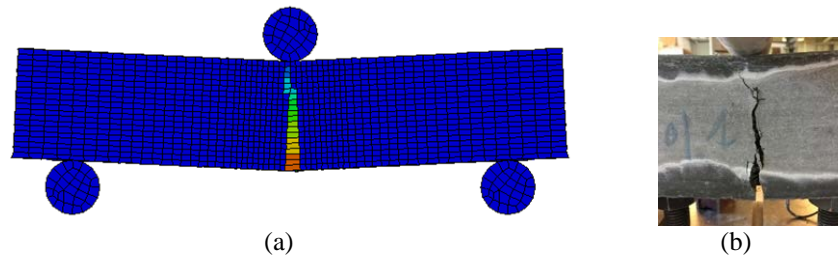


Fig. 2 Comparisons of flexural load-displacement curve



**Fig. 3 Comparison of crack pattern in the 2% fiber UHPFRC beam under bending:**  
 (a) numerical result, (b) experimental result

### 3.3 Numerical analysis of layer thickness effects

#### 3.3.1 Effects of layer thickness on load and energy

Layer thickness ratio  $\beta = h/H$  is defined to present the layer thickness changes, where  $H$  is the thickness of the whole beam and  $h$  is the thickness of the 2% UHPFRC layer. The flexural load-displacement curves of the double-layered beams with  $\beta = 0$  to 1 are shown in Fig. 4, in which  $\beta = 0$  and 1 represent the homogeneous UHPC and the 2% fiber UHPFRC beams respectively. The effects of the layer thickness ratio  $\beta$  on the peak flexural load  $F_{\max}$  and the energy  $E$  are depicted in Fig. 5. The fracture energy  $E$  is evaluated by the area under the flexural load-deflection curve up to a displacement of 0.01 m.

As can be observed in Fig. 5a, the peak flexural strength  $F_{\max}$  increases nonlinearly with the increase of the UHPFRC layer thickness when  $\beta$  changes from 0.1 to 1. Note that  $F_{\max}$  of the plain UHPC beam is higher compared to that of the 2% fiber UHPFRC beam, which is also observed in the experiments. This can be attributed to the lower water/binder ratio and better flowability of the UHPC mixture, resulting in a denser microstructure and hence a higher  $F_{\max}$ . The fracture energy  $E$  is also improved with the increase of  $\beta$ , as presented in Fig. 5b. This improvement tends to be more obvious when  $\beta$  is smaller than 0.7. Beyond this threshold, further increasing the UHPFRC layer thickness only results in limited energy enhancement, indicating an inefficient usage of the UHPFRC material.

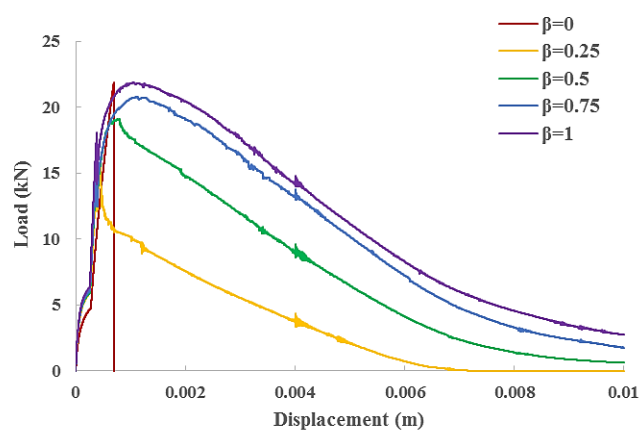


**Fig. 4 Flexural load-displacement curves with different layer thickness ratio  $\beta$**

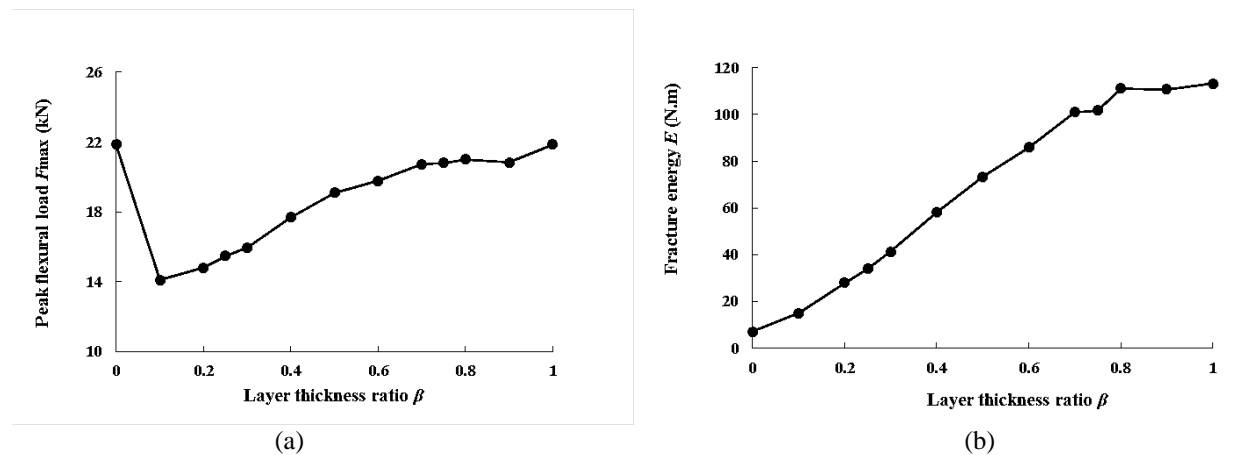


Fig. 5 Effects of the layer thickness ratio on: (a) peak flexural load, (b) fracture energy

### 3.3.2 Effects of layer thickness on stress distribution

Fig. 6 presents the stress distributions in the double-layered UHPFRC beams at  $t = 0.03$  h, which is still at the elastic stage. The blue color represents the tensile stress while the red color represents compression. It can be obtained from the figure that the stress distributions at the given moment are similar for the plotted beams although they have different layer thickness ratios. These results demonstrate that the layer thickness has insignificant effects on the stress distribution when the deformation of the beam is elastic.

In contrast, changing the layer thickness can affect the stress distribution in the beam when it is at the inelastic stage. The stress distribution at  $t = 0.3$  h is taken as an example and shown in Fig. 7. It can be observed that the tensile stress propagates upwards to the top surface of the beam at the given moment instead of concentrated near the beam bottom at  $t = 0.03$  h. This process shows the stress development in the double-layered beam with the applying of the load. Moreover, the tensile stress is more widely distributed in the beam with a thicker UHPFRC layer. This larger tensile region indicates a higher possibility of cracking and thus more consumed energy, which explains the increasing fracture energy dissipation with a larger layer thickness ratio (see Fig. 5b).

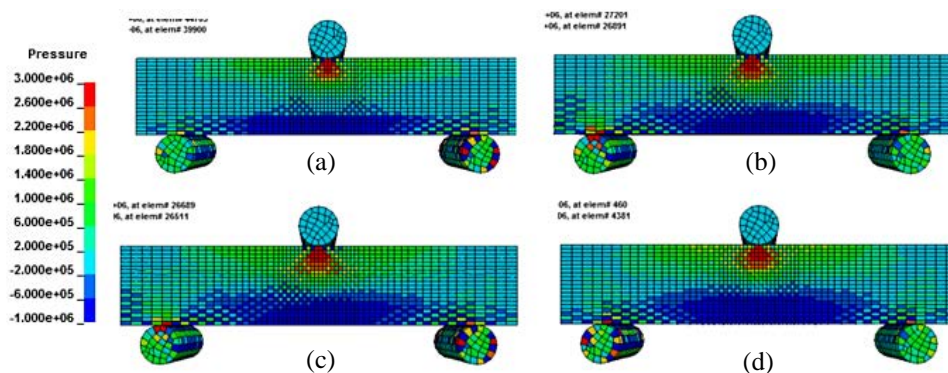


Fig. 6 Stress distribution in the beams at  $t = 0.03$  h: (a)  $\beta = 0.25$ , (b)  $\beta = 0.5$ , (c)  $\beta = 0.75$ , (d)  $\beta = 1.0$

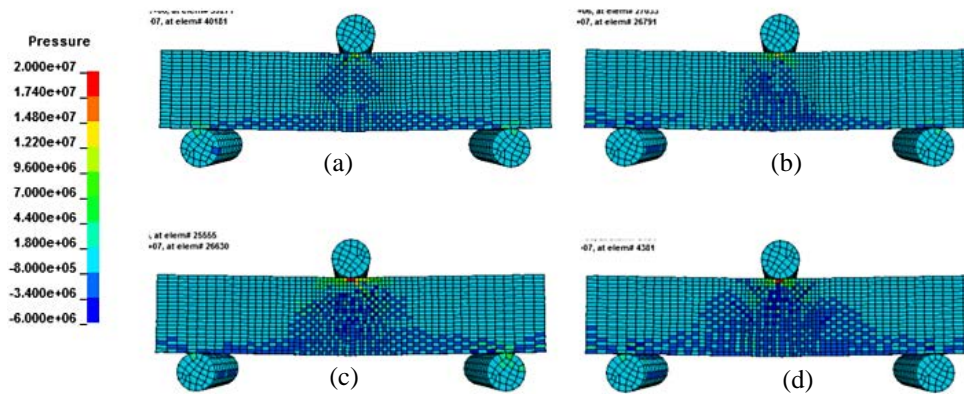


Fig. 7 Stress distribution in the beams at  $t = 0.3$  h: (a)  $\beta = 0.25$ , (b)  $\beta = 0.5$ , (c)  $\beta = 0.75$ , (d)  $\beta = 1.0$

#### 4. Conclusions

This study designed a double-layered UHPFRC beam with a plain UHPC layer at the top and a 2% fiber UHPFRC layer at the bottom. Experiments were conducted to test the basic properties of the UHPC and the UHPFRC materials, and the results were further used as inputs and validations for the modelling in the simulation section. Based on the validated model, flexural performances of double-layered UHPFRC beams were investigated numerically, and influences of the layer thickness ratio on the peak flexural load  $P_{\max}$ , the energy  $E$  and the stress distribution were analyzed. The results from this study shed lights on the design of layered UHPFRC structures, contribute to a more efficient utilization of steel fibers, as well as promote the technological application of layered UHPFRC in engineering constructions. The following conclusions can be drawn from the study:

- (1) Increasing the layer thickness ratio  $\beta$  from 0.1 to 1 leads to the increases of both  $P_{\max}$  and  $E$ . The improvement of  $E$  is more apparent when  $\beta$  is smaller than 0.7, beyond which the influence of layer thickness becomes limited.
- (2) The stress distribution in the double-layered UHPFRC beam under three-point bending is almost independent of the layer thickness when it is at the elastic stage. On the contrary, at the inelastic stage the tensile region increases with the increase of the layer thickness ratio.

#### 5. References

- [1] Yu R. Development of sustainable protective Ultra-High Performance Fibre Reinforced Concrete (UHPFRC). Eindhoven University of Technology, 2015.
- [2] Abbas S, Soliman AM, Nehdi ML. Exploring mechanical and durability properties of ultra-high performance concrete incorporating various steel fiber lengths and dosages. *Constr Build Mater* 2015;75:429–41. doi:10.1016/j.conbuildmat.2014.11.017.
- [3] YANG J, HAI R, DONG Y, WU K. Effects of the Component and Fiber Gradient Distributions on the Strength of Cement-based Composite Materials. *J Wuhan Univ Technol* 2003;18:61–4.

- [4] Yigiter H, Aydin S, Yazici H, Yardimci MY. Mechanical performance of low cement reactive powder concrete (LCRPC). *Compos Part B Eng* 2012;43:2907–14. doi:10.1016/j.compositesb.2012.07.042.
- [5] Bencardino F, Rizzuti L, Spadea G, Swamy RN. Experimental evaluation of fiber reinforced concrete fracture properties. *Compos Part B Eng* 2010;41:17–24. doi:10.1016/j.compositesb.2009.09.002.
- [6] Yoo DY, Kim S, Park GJ, Park JJ, Kim SW. Effects of fiber shape, aspect ratio, and volume fraction on flexural behavior of ultra-high-performance fiber-reinforced cement composites. *Compos Struct* 2017;174:375–88. doi:10.1016/j.compstruct.2017.04.069.
- [7] Kim DJ, Park SH, Ryu GS, Koh KT. Comparative flexural behavior of Hybrid Ultra High Performance Fiber Reinforced Concrete with different macro fibers. *Constr Build Mater* 2011;25:4144–55. doi:10.1016/j.conbuildmat.2011.04.051.
- [8] Comité Européen de Normalisation. Testing hardened concrete - Part 3: Compressive strength of test specimens. *Eur Stand EN 12390–3* 2009.
- [9] CEN. EN 12390-6:2000 Testing hardened concrete - Part 6: Tensile splitting strength of test specimens. 2000;44:1–8.
- [10] Test CC, Drilled T, Elements C, Drilled U, Cores C, Concrete C. Standard Test Method for Static Modulus of Elasticity and Poisson ' s Ratio of Concrete 2012:1–5. doi:10.1520/C0469-02E01.2.
- [11] Corinaldesi V, Nardinocchi A. Mechanical characterization of Engineered Cement-based Composites prepared with hybrid fibres and expansive agent. *Compos Part B Eng* 2016;98:389–96. doi:10.1016/j.compositesb.2016.05.051.
- [12] RILEM TC 162-TDF. Recommendations of RILEM TC 162-TDF: Test and design methods for steel fibre reinforced concrete: bending test. *Mater Struct* 2002;35:579–82. doi:10.1617/14007.
- [13] LSTC. Keyword User ' S Manual VOLUME II Material Models. vol. II. 2007. doi:10.1016/j.chemosphere.2011.02.019.
- [14] Dev L, Oftware LIS, Orporation TEC. Is-dyna Theory Manual. 2016th ed. California: Livermore Software Technology Corporation 7374; 2016.